

**NUMERICAL MODELING OF THE THERMAL STATE OF EARTH AFTER THE MOON-FORMING IMPACT EVENT.** L. Allibert<sup>1</sup>, N. Güldemeister<sup>1,2</sup>, L. Manske<sup>1,3</sup>, M. Nakajima<sup>4</sup>, K. Wünnemann<sup>1,3</sup>, <sup>1</sup>Museum für Naturkunde, Leibniz Institute for Evolution and Biodiversity Science, Berlin, Germany, (Laetitia.allibert@mf.n.berlin). <sup>2</sup>Department of Geosciences and Geography, University of Helsinki, Finland. <sup>3</sup>Freie Universität Berlin, Institute for Geological Science, Germany. <sup>4</sup>Department of Earth and Environmental Sciences, University of Rochester, USA.

**Introduction:** Planetary collisions play an important role in the compositional and thermal evolution of the planetary system. The final stage of planet formation is characterized by collisions of large bodies. The Moon-forming impact event is thought to be Earth's last giant collision event, marking the end of the main accretion phase of the Earth. This large event (re)set the conditions for the subsequent thermochemical evolution of both bodies, Earth and Moon. Large parts of proto-Earth are thought to melt as a consequence of the impact [e.g. 1] and the extent of melting affects the evolution of the Earth's interior and atmosphere. It is critical to address the initial conditions of the proto-Earth and the volume and shape of a possible magma ocean after the impact to understand the Earth's subsequent evolution.

To investigate the subsequent thermochemical evolution after the impact of a Mars-size object, and to quantify the volume of melt production, we carried out numerical simulations of the Moon-forming impact event considering different impact scenarios. Different impact conditions affect the amount of melting leading to either a global or partial magma ocean.

**Methods:** Previously, the Moon-forming giant impact was modeled with mesh-free so-called smoothed particle hydrodynamics (SPH [1, 2, 3]). In contrast, our new models are based on an ALE (Arbitrary-Lagrangian-Eulerian) code with a fixed grid in space which tend to be more accurate in the description of thermodynamics and shock waves. The three-dimensional (3D) iSALE code [4, 5] is used to model Moon-forming impact scenarios. iSALE accounts for multi-material and strength. We also compare simulation results from our iSALE code with SPH models for benchmarking ([1]). SPH uses self-gravity, whereas iSALE uses central gravity.

For the Moon-forming models, the core of proto-Earth is represented by the Analytical Equation of State (ANEOS, [6]) for iron and the mantle by ANEOS for dunite. We take into account two different initial thermal profiles [7] (cold and warm) for proto-Earth (Fig.1). The impactor has a dunitic material without an iron core. In all our simulations the impactor corresponds to a Mars-size object impacting onto proto-Earth. We vary the impact angle (15° to 90°) and impact velocities (12 to 20 km/s), systematically.

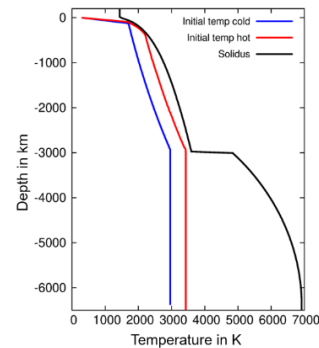


Figure 1: Thermal profile for a cold and warm Earth including a solidus function.

In order to quantify the volume of impact-induced melt, we use the so-called peak-shock pressure approach ('Tracer method') that has been used in several modeling studies [8,9] and is described in more detail by [10]. It is based on the assumption that the shock wave-induced increase in temperature is proportional to the maximum shock pressure the material experiences.

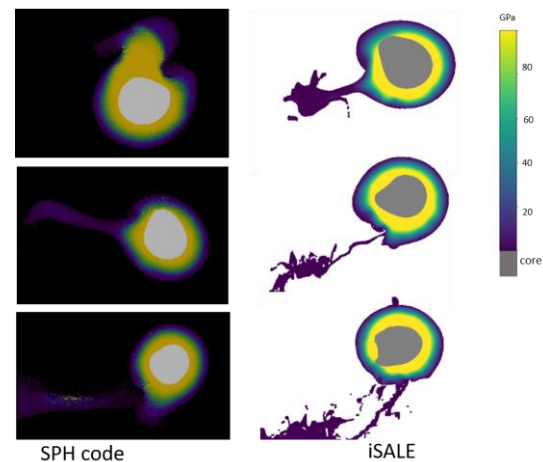


Fig. 2: Comparison of pressure evolution for a canonical Moon-forming impact event using two different numerical approaches: a mesh-free smooth particle hydrodynamics code (left), a grid-based Eulerian shock physics code iSALE (right).

**Results:** The benchmark study shows a good agreement of the two different numerical approaches with respect to pressure evolution as seen in Fig. 2. Here we consider a canonical impact scenario with a

moderate impact angle of  $41^\circ$  and an impact velocity of Earth's escape velocity. Previous SPH simulations suggest that the majority of mantle material experiences melting (between 68 and 80% mantle melting [1]) pointing to the existence of a global magma ocean with a base close to the core-mantle boundary in both impact scenarios [1]. The melt production obtained by the iSALE simulation is at least for the standard impact scenario smaller and only partial melting occurs in the canonical impact model.

Looking at the melt production in iSALE models for different Moon-forming impact scenarios the amount of melt decreases with decreasing impact angle (Fig. 3). For all impact angles a global magma ocean is observed. The depth of the magma ocean increases with increasing impact angle. Melting reaches the core-mantle boundary for impacts at angles  $>45^\circ$ .

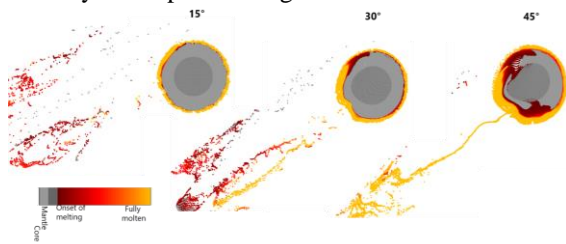


Fig. 3: Melt production and distribution for a Moon-forming impact event of impact velocity 15km/s and a warm initial profile, considering different impact angles ranging from very shallow to the most likely case of a  $45^\circ$  impact angle.

Figure 4 illustrates the melt efficiency for the different scenarios as a function of impact angle. The melt efficiency is given by the melt volume normalized by the projectile volume. The presented results show that not only with increasing impact angle but also with increasing impact velocity and warmer thermal conditions, melt production increases. The effect of the pre-impact temperature is more pronounced for impacts at steeper angles. The volume of melt decreases by about 60% for impacts from  $45^\circ$  down to  $15^\circ$ , which is consistent with data from [11]. For a  $45^\circ$  impact angle, in all scenarios, 20% of mantle material is molten and about 50% of mantle melting occurs for the warm and fastest impact scenario.

Our models suggest that in impact scenarios with impact angles  $>15^\circ$  at 12km/s ( $\sim$  escape velocity) a global magma ocean is formed although complete melting of the mantle is unlikely.

The presence of the Earth's core has a limiting effect on the melt production as simulations without a core have shown (not shown here).

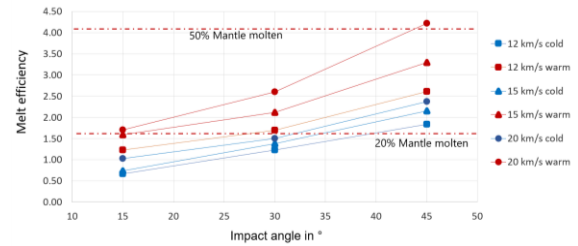


Fig. 4: Melt efficiency (Melt volume per projectile volume) as a function of impact angle for the impact scenarios varying the initial thermal profile of Earth and the impact velocity ranging from 12 to 20 km/s.

**Conclusion/Discussion:** Numerical simulations of Moon-forming impact scenarios allow for quantifying the melt production as a function of impact angle, velocity and initial thermal state. In all our simulations the Moon-forming impact scenarios produce a global magma ocean. A warm proto-Earth, larger impact angles and larger impact velocities, produce a larger amount of melt and melt distribution can reach the core of proto-Earth. As iSALE neglects the presence of an impactor core, this will underestimate melt production assuming differentiated impactors would increase melting.

In future work we will consider the additional heating by plastic work and include self-gravity in our simulations. We will also take into account differentiated impactors and track the fate of the impactor's core in the course of crater formation. Of particular interest is how the impactor core is dispersed in Earth's mantle and how much impactor and target material is ejected and may even escape the Earth-Moon system.

**Acknowledgments:** We gratefully thank the iSALE developers, including Gareth Collins, Kai Wünnemann, Dirk Elbeshausen, Boris Ivanov and Jay Melosh and Thomas Davison for the development of the pysaleplot tool. We also thank the Deutsche Forschungsgemeinschaft (SFB-TRR 170, subproject C2 and C4) for funding.

**References:** [1] Nakajima M. and Stevenson D. J. (2015) EPSL, 427, 286-295. [2] Canup R. M. et al. (2013) ICARUS 222, 200-219. [3] Canup R. M. (2004) Science 338, 1052-1054. [4] Collins G. S. et al. (2004) Meteoritics & Planet. Sci., 39, 217-231. [5] Wünnemann K. (2006) ICARUS 180, 514-527. [6] Thompson S. L. (1990) Technical Report SAND89-2951 UC-404, 76 pages. [7] Plesa, A.-C. et al. (2016) JGR 121, 2386-2403. [8] Wünnemann K. et al. (2008) EPSL 269, 529-538. [9] Pierazzo et al. (1997) ICARUS 127, 408-423. [10] Manske L. et al. (2018) 49th LPSC, abstract# 2269. [11] Pierazzo and Melosh (1999) EPSL 165, 163-176.